Journal of Computational Physics 229 (2010) 3664–3674

Contents lists available at ScienceDirect

Journal of Computational Physics

journal homepage: www.elsevier.com/locate/jcp

Coupling *p*-multigrid to geometric multigrid for discontinuous Galerkin formulations of the convection–diffusion equation

Brendan S. Mascarenhas [a,*], Brian T. Helenbrook [b], Harold L. Atkins [c]

[a] Optiwind LLC, 59 Fields St., Torrington, CT 06790, USA
[b] Mechanical and Aeronautical Engineering Department, Clarkson University, Potsdam, NY 13699-5725, USA
[c] Computational AeroSciences Branch, NASA Langley Research Center, MS 128, Hampton, VA 23681-2199, USA

ARTICLE INFO

Article history:
Received 1 December 2008
Received in revised form 27 July 2009
Accepted 19 January 2010
Available online 1 February 2010

Keywords:
p-Multigrid
Geometric multigrid
Discontinuous Galerkin
Convection–diffusion equation

ABSTRACT

An improved *p*-multigrid algorithm for discontinuous Galerkin (DG) discretizations of convection–diffusion problems is presented. The general *p*-multigrid algorithm for DG discretizations involves a restriction from the $p = 1$ to $p = 0$ discontinuous polynomial solution spaces. This restriction is problematic and has limited the efficiency of the *p*-multigrid method. For purely diffusive problems, Helenbrook and Atkins have demonstrated rapid convergence using a method that restricts from a discontinuous to continuous polynomial solution space at $p = 1$. It is shown that this method is not directly applicable to the convection–diffusion (CD) equation because it results in a central-difference discretization for the convective term. To remedy this, ideas from the streamwise upwind Petrov–Galerkin (SUPG) formulation are used to devise a transition from the discontinuous to continuous space at $p = 1$ that yields an upwind discretization. The results show that the new method converges rapidly for all Peclet numbers.

1. Introduction

The *p*-multigrid (synonymously spectral multigrid [1], hierarchic multigrid [2], or multi-level method [3]) algorithm originally proposed by Rönquist and Patera [1] is an iterative technique to solve *hp*-finite element discretizations of equations. After a dormant period of more than a decade, the method has received renewed interest in recent works by Helenbrook et al. [4], Helenbrook and Atkins [5,6], Fidkowski et al. [7], Oliver [8] and Luo et al. [9]. The *p*-multigrid method consists of a 'multigrid-like' algorithm with levels coarsened by reducing the order of the approximating polynomial, *p*. For example, to solve equations derived using polynomials of order 4, relaxations could be performed on solution approximations of order 4, 2, 1 and then 0. When a low polynomial degree is reached, one can use standard techniques such as geometric multigrid, GMRES, or direct inversion to solve the remaining smaller system of equations.

While *p*-multigrid is generally effective, recent work by Helenbrook and Atkins [5] has shown that for discontinuous Galerkin (DG) formulations of diffusive problems, the performance of the algorithm degrades when coarsening from $p = 1$ to $p = 0$. We have also observed a similar difficulty in applications of *p*-multigrid to DG discretizations of the 2-D Euler equations [10]. Helenbrook and Atkins [6] discovered the underlying reason for this degradation and provided a correction that works well for diffusive problems. In this work, we show that their correction fails when applied to problems that include convective transport. We explain this failure and present a new method to overcome the difficulty.

* Corresponding author.
E-mail addresses: bmascarenhas@optiwind.com (B.S. Mascarenhas), helenbrk@clarkson.edu (B.T. Helenbrook), harold.l.atkins@nasa.gov (H.L. Atkins).

0021-9991/$ - see front matter © 2010 Elsevier Inc. All rights reserved.
doi:10.1016/j.jcp.2010.01.020

2. The steady convection–diffusion equation

The one dimensional, steady CD equation in conservation form is:

$$\frac{d}{dx}(a\,w+\sigma)=f(x) \tag{1}$$

$$\sigma=-\kappa\frac{dw}{dx} \tag{2}$$

where w is the steady solution, a is the convective wave velocity (assumed constant), κ is the diffusivity (assumed constant), f is a source function and σ is the diffusive flux. Because the source function, f, does not affect the convergence of a numerical scheme, we neglect it in further analysis. We study this problem on a domain with periodic boundary conditions.

2.1. The discontinuous Galerkin formulation

To formulate the discrete problem, the domain is subdivided into N elements of uniform length, and on each element, we use a polynomial basis to describe the solution, w_h, and the diffusive flux σ_h. The subscript h refers to the element length. Following the notation in Arnold et al. [11], we define the following space of functions to represent the solution:

$$U_h := \{u \in L^2(\Omega) : u|_K \in \mathcal{P}_p(K)\ \forall K \in \mathcal{T}_h\} \tag{3}$$

where $L^2(\Omega)$ is the space of square-integrable functions on the domain Ω. $\mathcal{T}_h$ is the set of segments K that span the domain. $\mathcal{P}_p(K)$ is the space of polynomial functions of degree at most p on segment K.

All the DG formulations analyzed are based on the weak form of Eqs. (1) and (2). Multiplying these equations by test functions $v_h,\ \tau_h \in \mathcal{P}_p(K)$, respectively, and integrating by parts gives the weak form which is used to find $w_h \in U_h$ and $\sigma_h \in U_h$

$$-\int_{x_{k-1}}^{x_k}(aw_h+\sigma_h)\frac{dv_h}{dx}\,dx=-(\widehat{aw}+\hat{\sigma})v_h\big|_{x_{k-1}}^{x_k}\quad \forall v_h \in \mathcal{P}_p(K) \tag{4}$$

$$\int_{x_{k-1}}^{x_k}\left(\sigma_h\tau_h-w_h\frac{d\tau_h}{dx}\right)dx=-\hat{w}\tau_h\big|_{x_{k-1}}^{x_k}\quad \forall \tau_h \in \mathcal{P}_p(K) \tag{5}$$

where x_{k-1} and x_k are the left and right boundary, respectively, of element K. $\widehat{aw}$, $\hat{\sigma}$, and $\hat{w}$ are boundary flux functions. These functions are evaluated at element boundaries using information from both sides of the element and thus provide the inter-element coupling in a DG scheme.

The schemes for evaluating the diffusive fluxes, $\hat{\sigma}$ and $\hat{w}$, that are investigated here are listed in Table 1. The notation follows that of Arnold et al. [11]: braces $\{\}$ denote the average of a quantity at an element boundary. Double brackets $[\![\,]\!]$ denote the jump in a quantity at an element boundary. In the LDG scheme, the constant β can take values between $-1/2$ and $1/2$. The constant α_j is given by ηh^{-1}, where η is an $O(1)$ constant . We present results for only the LDG scheme with $\beta=0$ and a baseline value of $\eta=4$. For the Bassi–Rebay scheme, $\alpha_r([\![u_h]\!])$ is defined by a "lifting operator" [11] and again has an adjustable constant, η. The baseline value of η is 1. In the results, η is varied to understand the sensitivity to this parameter. In this case η_0 will denote the baseline value ($\eta_0=4$ for the LDG $\beta=0$ scheme, and $\eta_0=1$ for the Bassi–Rebay scheme).

The convective flux, $\widehat{aw}$, is evaluated using an upwind scheme as

$$\widehat{aw}=a\{w_h\}-\frac{|a|}{2}[\![w_h]\!] \tag{6}$$

3. The block Jacobi relaxation scheme

Before describing the relaxation scheme, we introduce some matrix notation for the discrete equations obtained from the DG formulation. The vector of solution coefficients for element j is given by w_j . The solution on this element is represented as $\phi^T w_j$ where ϕ is the vector of polynomial basis functions spanning $\mathcal{P}_p(K)$. The vector of coefficients and basis functions for an element is of length $p+1$.

The block Jacobi iterative scheme can be written in the form

$$R\Delta w+(Aw-S)=0 \tag{7}$$

Table 1
DG schemes analyzed and their numerical fluxes.

Scheme	$\hat{w}$	$\hat{\sigma}$
Local DG (LDG) [12]	$\{w_h\}-\beta\cdot[\![w_h]\!]$	$\{\sigma_h\}+\beta[\![\sigma_h]\!]-\alpha_j[\![w_h]\!]$
Bassi et al. [13]	$\{w_h\}$	$\{\nabla_h w_h\}-\alpha_r([\![w_h]\!])$

where R is a relaxation matrix, w is the vector of unknown coefficients for all elements, A is the stiffness matrix. A block is defined as the matrix of coefficients of the discrete equations for an individual element. Each block is of size $(p+1)\times(p+1)$. For the block Jacobi scheme, R is the block on the diagonal of A. We also introduce an under-relaxation parameter ω. ω scales the magnitude of the diagonal blocks of the relaxation matrix by a factor of $\frac{1}{\omega}$. Hence, a smaller value for ω corresponds to reducing the magnitude of the correction applied at each iteration.

4. Multigrid

p-Multigrid is used to accelerate convergence of the relaxation scheme. As in a standard multigrid algorithm, in p-multigrid, restriction and prolongation operators are needed in addition to the relaxation scheme. For $p>1$, the restriction operation consists of moving solution residuals from a space of high polynomial order to a lower order. Based on the order of the coarse space polynomial there are different p-multigrid strategies. The most frequently used algorithms employ a coarse space polynomial order of either $p_c = p/2$ [5,6,10], $p_c = p-1$ [14,15], or $p_c+1=(p+1)/2$ [16]. Helenbrook and Atkins [6] have compared these algorithms for the Poisson equation and their results show that $p_c = p-1$ offers only a small improvement over $p_c = p/2$. Also, there is no consistent trend to indicate any advantage to using $p_c+1=(p+1)/2$ over $p_c = p/2$. Hence either method is functional. To maintain consistency with our earlier work, we have chosen to use $p_c = p/2$. When $p=1$, standard p-multigrid restriction moves the solution residuals to a discontinuous space of constants i.e. $p=0$. Prolongation is the reverse operation in which the solution correction from the low-order space is transferred to the higher-order space. For a basis ϕ_c of degree p_c that is contained in the space spanned by a higher-order basis, ϕ of degree p, the prolongation operator on an element is given by

$$I_{l,l+1} = \left(\int_K \phi\phi^T dx\right)^{-1} \int_K \phi\phi_c^T dx \tag{8}$$

The subscript l indicates the multigrid level: $l=0$ corresponds to the finest level. The above matrix is of dimension $(p+1)\times(p_c+1)$ and takes a correction represented using the basis ϕ_c and gives an equivalent representation using the basis ϕ. In this work, we use a nodal basis which is not hierarchical. Prolongation is essentially a correction applied to the low-order terms while keeping the high-order terms unchanged. The restriction operator is the transpose of prolongation. This corresponds to transferring only the residuals derived from integration with respect to the low-order terms of the approximating polynomials to the coarser space. When a low value of p is reached, one is left with a system of equations which has a small number of unknowns per element. For example, if $p=0$, there is one unknown per element, and the system is similar to a cell-centered finite volume system.

The multigrid algorithm in a V-cycle can be written as a recursive subroutine as follows:

```
cycle(l) {
  if (l != coarsest level) {
  Direct inversion on coarse mesh:
    w_[l] = A_[l]^-1 (S_[l])
    return
  }
  Relaxation:
    w_[l] = w_[l] + R_[l]^-1 (S_[l] - A_[l] w_[l])
  Restriction:
    S_[l+1] = I^T_{l,l+1} (S_[l] - A_[l] w_[l])
    w_[l+1] = 0
  Recursion:
    cycle(l + 1)
  Prolongation:
    w_[l] = w_[l] + I_{l,l+1} w_[l+1]
  return
}
```

The subscript $[l]$ again indicates the multigrid level with $l=0$ corresponding to the finest level. $w_{[0]}$ is the solution to the discrete CD equation. For higher values of l, $w_{[l]}$ is a solution correction that will be prolongated to a higher-order space. $S_{[l]}$, for $l=0$ is the vector of source terms in the governing equations on the finest mesh ($S_{[0]}=0$ from Section 2), and on the coarser meshes, i.e. for $l>0$, it is the restriction of the residual from the previous level. For $l=0$ to $l=1+\log_2(p_{[0]})$ the algorithm is the p-multigrid algorithm where $p_{[0]}$ is the value of p used for the simulation. For example, for $p_{[0]}=4$, level 0, 1, 2, and 3 would have $p=4,2,1$, and 0, respectively. For these levels the prolongation and restriction operators are determined using Eq. (8). At the coarsest level, the matrix equations are directly inverted. The two-level cycle iteration gives an upper bound for the convergence rate because the second level equations are solved directly rather than iteratively. To be consistent with our earlier analyses on the subject [5,6,10], the above V-cycle incorporates a single pre-smoothing step and no post-smoothing We have verified that adding additional relaxations (smoothing) does not change the qualitative conclusions.

For the p-multigrid levels of the iteration, the stiffness matrices $A_{[l]}$ at the coarse levels are determined using an "algebraic" approach. In this approach, the coarse level stiffness matrices are evaluated using the restriction and prolongation operators

$$A_{[l+1]} = I_{l,l+1}^T A_{[l]} I_{l,l+1} \tag{9}$$

Helenbrook and Atkins [5], have shown that this technique is more reliable and usually gives better results than the "rediscretization" approach in which the coarse matrices are formed by obtaining the DG formulation of the problem on the coarser space.

5. Analysis techniques

For the analysis, we assume that the source function S is zero because the source term does not affect convergence. To determine the convergence rates, we examine the eigenvalues of the multigrid iteration. For the two-level iteration we use here, one multigrid cycle can be simplified to the following form:

$$w^{[1]} = \left(I - I_{0,1} A_{[1]}^{-1} I_{0,1}^T A_{[0]}\right)\left(I - R_{[0]}^{-1} A_{[0]}\right) w^{[0]} \tag{10}$$

where I is the identity matrix. The spectral radius of the above matrix determines the damping factor, which is the amount that the error is decreased in each multigrid cycle. A damping factor less than one indicates that the scheme is convergent (stable), whereas a scheme is nonconvergent if it has a damping factor greater than or equal to one. A stable scheme converges more rapidly if its damping factor is closer to zero.

The continuous problem has periodic boundary conditions hence the matrices are circulant and we can use the discrete Fourier transform to reduce the size of the matrix. We assume the solution on each element has the form:

$$w_j = \tilde{w}_j e^{ik\theta} \tag{11}$$

where j is the element index, $\tilde{w}_j$ is a vector of dimension $(p+1)$ and θ can take values of $-\pi$ to π by increments of $2\pi/N$ where N is the number of linear elements. Substitution of the form given by Eq. (11) reduces the eigenvalue problem of size $N(p+1)$ to a set of N eigenvalue problems of size $(p+1)$. These are then solved numerically for each value of θ. $\theta = 0$ is excluded from the analysis because on a periodic domain this corresponds to a mode which is determined only up to a free constant and is undamped for any scheme. The maximum eigenvalue over the range $-\pi < \theta < \pi$ is the damping factor of the iterative scheme.

6. Review of Poisson equation results

To illustrate the failure of p-multigrid when coarsening from $p = 1$ to $p = 0$, we present some results similar to earlier work by Helenbrook and Atkins [5,6] on the application of p-multigrid to the DG formulations of Poisson's equation described in Section 2.1. Table 2 shows the 1D damping factors obtained using block Jacobi relaxation combined with 2-level p-multigrid. Notice that the damping factors for the $p = 1$ to 0 case are closer to one (slower converging) than most of the other entries in the table especially when $\eta/\eta_0 = 4$. With $\omega = 2/3$, the damping factors for $p = 1$ to 0 are essentially the same as those in Table 2. We observed a similar difficulty with the $p = 1$ to 0 transition in our study of p-multigrid solution methods for DG discretizations of the 2D Euler equations [10]. This apparently anomalous behavior of the $p = 1$ to $p = 0$ transition is problematic because it consequently limits the convergence rate of any cycle that coarsens to $p = 0$. Helenbrook and Atkins [6] have shown that the reason the $p = 1$ to 0 iteration fails is that the slowly damped modes of the $p = 1$ relaxation are essentially continuous functions. These functions cannot be represented well in the $p = 0$ (coarse) space and thus the damping by multigrid is poor. For the higher-order p-multigrid transitions, such as the $p = 2$ to 1, both spaces, fine and coarse, can represent continuous functions well, so this difficulty does not occur.

Table 2
1D damping factors for a 2-level block Jacobi iteration between various levels of p and with $\omega = 2/3$.

Scheme	p	η/η_0 = 1	η/η_0 = 4
LDG, $\beta = 0$	1–0	0.79	0.93
Bassi et al.	1–0	0.61	0.85
LDG, $\beta = 0$	2–1	0.52	0.39
Bassi et al.	2–1	0.66	0.39
LDG, $\beta = 0$	4–2	0.67	0.46
Bassi et al.	4–2	0.74	0.39
LDG, $\beta = 0$	8–4	0.86	0.65
Bassi et al.	8–4	0.84	0.40

The problem with p-multigrid at $p = 1$ can be corrected for pure diffusion by coarsening from a first order, discontinuous polynomial (fine) space to a first order, continuous polynomial (coarse) space. In the discontinuous $p = 1$ space, the basis consists of the two functions

$$\phi = \begin{bmatrix} (1-\xi)/2 \\ (1+\xi)/2 \end{bmatrix} \tag{12}$$

where ξ is a local coordinate on the element which goes from -1 to 1 across the element. At the next level of multigrid, we enforce continuity of these functions across element boundaries. Thus, there will be one piecewise-linear, continuous function associated with each vertex in the 1D mesh. This is exactly the basis that is typically used in continuous linear finite element formulations. In the continuous space, the number of degrees of freedom per element is 1 so this corresponds to halving the number of degrees of freedom in the approximation space.

If we choose the convention that, in the continuous space, the left vertex is the degree of freedom associated with each element; the restriction operator for the transition from the $p = 1$ discontinuous to continuous space for element K is given by

$$\begin{aligned} I^T_{C-D_{K,K-1}} &= [0 \quad 1] \\ I^T_{C-D_{K,K}} &= [1 \quad 0] \\ I^T_{C-D_{K,K+1}} &= [0 \quad 0] \end{aligned} \tag{13}$$

where $I^T_{C-D_{K,K-1}}$ is the block of the discontinuous-to-continuous restriction operator that multiplies the residuals on element $K-1$ to form the residual in the continuous space on element K. Basically, all contributions to the continuous residual at a given vertex are summed. For example, the residual restriction for element K consists of summing the contribution of the discontinuous residual associated with the right vertex function, $(1+\xi)/2$, on element $K-1$ with the corresponding component associated with the left vertex function, $(1-\xi)/2$, on element K. The prolongation operator is the transpose of this operation. This corresponds to applying the correction found for a vertex in the continuous space to both the left and right vertex functions in the linear discontinuous space.

Table 3 reproduces the results obtained by Helenbrook and Atkins using this transition. Comparing these results with the $p = 1$ results in Table 2, we see that the multigrid convergence rates have improved considerably. Hence, the transition to continuous space at $p = 1$ effectively solves the problem for Poisson's equation.

7. Convection–Diffusion equation

Inspired by this success, next we apply these ideas to DG discretizations of the steady CD equation. The behavior of the convection–diffusion equation is characterized by the magnitude of convective versus diffusive transport as characterized by the Peclet number, $Pe_h \equiv \frac{ah}{2\kappa}$. Hence, we study cases with Peclet number ranging from 10^{-3} (diffusion dominated) to 10^3 (convection dominated).

Fig. 1 shows the damping factors versus Pe_h for the Bassi et al. and LDG, $\beta = 0$ diffusive schemes when combined with the upwind convective scheme for a multigrid transition from a $p = 1$ discontinuous space to a $p = 1$ continuous space. The circular markers (○) are for the Bassi et al. scheme and the square markers (□) are for the LDG scheme. The schemes are shown for $\eta/\eta_0 = 1$. The results with $\eta/\eta_0 = 4$ are similar. The broken horizontal line at $y = 1$ indicates graphically the level below which the damping factors must lie for a scheme to be stable. For the diffusion dominated cases, both schemes perform well. However, as the magnitude of the convective transport becomes significant, the performance of the schemes degrade until they no longer converge.

7.1. The first order wave equation

To explain this failure, we turn our attention to the first order wave equation. We first analyze results obtained by p-multigrid transition from discontinuous $p = 1$ space to a continuous $p = 1$ space. Table 4 compares these results with the damping factors obtained using standard p-multigrid with $p = 1$ to 0 and $p = 2$ to 1 discontinuous spaces. Consistent with Fig. 1, transitioning to a continuous space at $p = 1$ is unstable. In contrast to the diffusive problem, p-multigrid performs well when coarsening from $p = 1$ to $p = 0$ for the wave equation. However, as we have indicated in the introduction, this is not true with more complicated systems such as the Euler equations. In order to develop an iterative method which works well for all Pec-

Table 3
1D damping factors for 2-level block Jacobi iteration, transitioning from a discontinuous $p = 1$ space to a continuous $p = 1$ space and with $\omega = 2/3$.

Scheme	η/η_0	
	1	4
LDG, $\beta = 0$	0.43	0.37
Bassi et al.	0.33	0.33

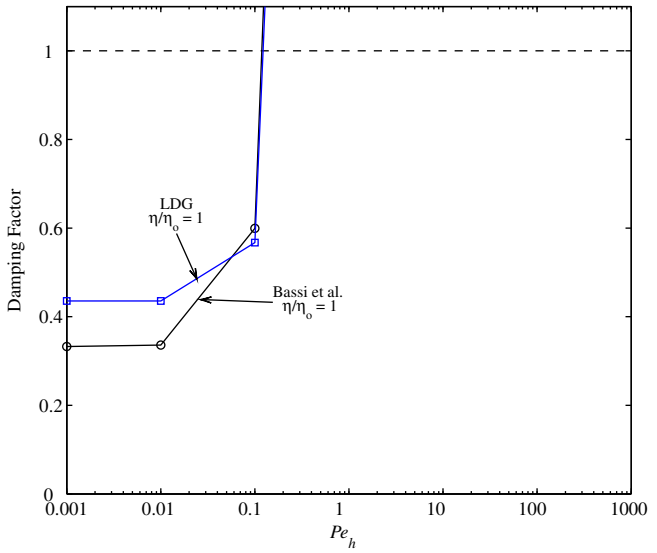

Fig. 1. Damping factors for the CD equation using a transition from $p = 1$ discontinuous space to $p = 1$ continuous Galerkin space, $\omega = 2/3$.

Table 4
Damping factors for variants of p-multigrid with the block Jacobi relaxation on a DG discretization of the 1-D first order wave equation.

p-Multigrid scheme	Damping factor
$p = 1$ discontinuous to $p = 0$ discontinuous	0.3333
$p = 1$ discontinuous to $p = 1$ continuous	Unstable
$p = 2$ discontinuous to $p = 1$ discontinuous	0.3333

let numbers and for systems, it is important to understand why the $p = 1$ discontinuous to continuous transition fails for the wave equation.

To explain why coarsening to a continuous space at $p = 1$ does not work, we first examine the outcome of applying the weighted-integral DG formulation as given by Eq. (14) to a continuous space. For the wave equation, this is given by

$$\sum_{k=1}^{N}\left[\int_{x_{k-1}}^{x_k} a w_h \frac{dv_h}{dx}\,dx - (\widehat{aw})\,v_h\big|_{x_{k-1}}^{x_k}\right] = 0 \quad \forall v_h \in U_h \cap C^0 \tag{14}$$

where w_h is also obtained from the continuous space $U_h \cap C^0$. The sum over all elements was not necessary in DG because the constraints could be applied element by element. We have summed the constraints to make the following point. Because w_h and v_h are continuous, the inter-element boundary terms in the sum cancel out leaving

$$\sum_{k=1}^{N}\int_{x_{k-1}}^{x_k} a w_h \frac{dv_h}{dx}\,dx - (\widehat{aw})\,v_h\big|_{x_0}^{x_N} = 0 \quad \forall v_h \in U_h \cap C^0 \tag{15}$$

This is exactly the continuous Galerkin formulation of convection. For first order polynomial approximations, the Galerkin formulation reduces to a central-difference approximation to the differential equation. Hence the discrete problem is no longer upwinded in the coarse continuous space thus causing the method to fail.

In our case, the coarse grid equations are not obtained by a weighted-integral method, but rather by using the restriction and prolongation operators. However, due to the summation involved, this also results in a central-difference formulation. To see this, Eq. (16) shows the $p = 1$ discontinuous formulation which is upwinded for $a > 0$. k_r is entirely 0 which indicates that there is no coupling to the downwind element.

$$K_{DG} = \begin{bmatrix} \ddots & \ddots & \ddots & & \\ & k_l & k & k_r & \\ & & \ddots & \ddots & \ddots \end{bmatrix}_{2N\times 2N} \tag{16}$$

where

$$k_l = \begin{bmatrix} 0 & -1 \\ 0 & 0 \end{bmatrix}, \quad k = \begin{bmatrix} 0.5 & 0.5 \\ -0.5 & 0.5 \end{bmatrix}, \quad k_r = \begin{bmatrix} 0 & 0 \\ 0 & 0 \end{bmatrix}$$

We next apply the restriction and prolongation operators to form the coarse grid stiffness matrix as shown in Eq. (17).

$$K_{coarse} = I^T \cdot K_{DG} \cdot I = \begin{bmatrix} \ddots & \ddots & \ddots & & \\ & -0.5 & 0 & 0.5 & \\ & & \ddots & \ddots & \ddots \end{bmatrix}_{N\times N} \tag{17}$$

where the restriction operator shown below restricts from the discontinuous to continuous space as discussed earlier.

$$I^T = \begin{bmatrix} \dots & 0 & 1 & 1 & 0 & \dots & \\ & \dots & 0 & 1 & 1 & 0 & \dots \end{bmatrix}_{N\times 2N}$$

Eq. (17) shows that the coarse grid equations obtained by using the restriction and prolongation operators is also a central-difference scheme. It is well-known that the central-difference equations are singular or very close to singular [17–19]. Thus, the p-multigrid iteration is unstable.

7.2. The streamwise upwind Petrov–Galerkin formulation

To avoid the problems associated with central-difference discretizations, we apply ideas from the streamwise upwind Petrov–Galerkin (SUPG) formulation [18] which gives an upwind discretization when the solution space is continuous. For the homogeneous 1D wave equation, the weak form of the SUPG formulation is given by

$$\sum_{k=1}^{N} \int_{x_{k-1}}^{x_k} \left(v_h + a\tau \frac{dv_h}{dx} \right) a \frac{dw_h}{dx}\, dx = 0 \quad \forall v_h \in U_h \cap C^0 \tag{18}$$

Here, the trial function w_h is also chosen from the continuous space $U_h \cap C^0$. Note that the weighting function is $v_h + a\tau \frac{dv_h}{dx}$ as opposed to just v_h as in a standard Galerkin formulation. The parameter τ is defined as $\frac{h}{2\cdot|a|}$. The term $a\tau \frac{dv_h}{dx}$ is responsible for providing the upwinding and is shown for $a > 0$ along with the standard Galerkin weighting function v_h in Fig. 2(a). The sum of those two functions is the SUPG weighting function and is shown in Fig. 2(b).

To improve the performance of p-multigrid, we direct our efforts towards developing a method to transition from a $p = 1$ DG discrete problem to a continuous SUPG discretization keeping p equal to 1. The restriction operator can be defined by finding the linear combination of fine grid weighting functions that form the coarse grid weighting functions. Based on Fig. 2(b), we can select the weights by which the fine space residuals are to be multiplied and then added together to give a coarse system that is equivalent to multiplying by the SUPG weight function and integrating. The restriction operator constructed to do this is shown in Eq. (19).

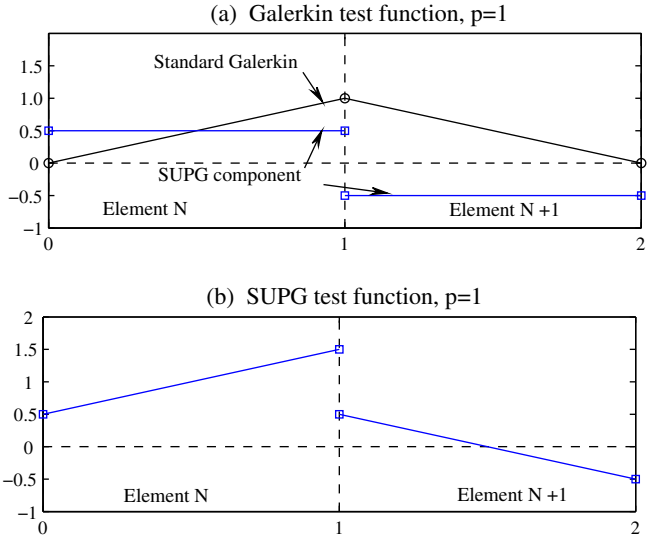

Fig. 2. (a) Standard Galerkin piecewise-linear weighting function v_h and SUPG component obtained from $a\tau(dv_h/dx)$. (b) Linear SUPG weighting function obtained by summing Galerkin and SUPG component $\left(v_h + a\tau \frac{dv_h}{dx}\right)$.

$$I^T_{SUPG} = \begin{bmatrix} \dots & 0 & [\cdots & \mathbf{V} & \cdots &] & 0 & \dots & \\ & \dots & 0 & [\cdots & \mathbf{V} & \cdots &] & 0 & \dots \end{bmatrix}_{N\times 2N} \tag{19}$$

where $[\cdots \quad \mathbf{V} \quad \cdots] = [0.5 \quad 1.5 \quad 0.5 \quad -0.5]$

Prolongation operators can be defined in a similar way to restriction operators except using the trial functions, not the weighting functions. Because the trial functions in SUPG are the same as in a standard Galerkin formulation, we use the same prolongation operator I, defined in Eq. (17) which was used to prolongate from the $p = 1$ continuous space to the $p = 1$ discontinuous space.

Using the new SUPG restriction and our previous prolongation operator, we can form the coarse grid matrices as was done previously. From Eq. (20) we see that by using this modified restriction operator, the resulting coarse space stiffness matrix gives a first order upwind discretization.

$$K_{upwind} = I^T_{SUPG} \cdot K_{DG} \cdot I = \begin{bmatrix} \ddots & \ddots & \ddots & & \\ & -1 & 1 & 0 & \\ & & \ddots & \ddots & \ddots \end{bmatrix}_{N\times N} \tag{20}$$

7.3. DG to SUPG results for the first order wave equation

There are two ways to incorporate the above modifications into the p-multigrid algorithm. In both implementations, upwind coarse grid equations are used. The coarse space equations can be obtained either algebraically using the upwind restriction operator and original prolongation operator as shown above or by SUPG rediscretization. Both methods give the same results which is a first order upwind discretization. Both methods also use the same prolongation operator. The difference between the two implementations is whether we use the SUPG restriction operator or the standard restriction operator to transfer the residuals to the coarse grid. If we use the standard restriction operator, this corresponds to a rediscretization approach using an upwind discretization. Upwind transfer operators have been used for geometric multigrid[20,21], however, as far as we are aware the method has not been attempted with p-multigrid.

The results of numerical experiments on the model problem using both implementations are shown in Table 5 for both implementations, along with the $p = 1$ to 0 p-multigrid result. If we use the SUPG residual restriction, the iteration converges rapidly at nearly the same rate as the $p = 1$ to 0 p-multigrid result. The use of standard restriction and prolongation to transfer residuals, but with an upwind discretization on the coarse grid, does not give good results. This indicates that not only does one need stable coarse grid operators, but also that these operators must be compatible with the restriction and prolongation methods. Because the damping factor obtained with the standard restriction is poor, we do not include this implementation in any of the following analyses.

7.4. DG to SUPG for the convection–diffusion equation

We now have effective methods for the diffusion equation and the wave equation. These two methods must be combined for application to the convection–diffusion equation. For this we again follow ideas from the SUPG formulation for the CD equation obtained by Brooks and Hughes [18]:

$$\sum_{k=1}^{N} \int_{x_{k-1}}^{x_k} \left(v_h + a\tau \frac{dv_h}{dx} \right) \left(a \frac{dw_h}{dx} - \frac{d^2 w_h}{dx^2} \right) dx = 0 \quad \forall v_h \in U_h \cap C^0 \tag{21}$$

where

$$\tau = \frac{\Delta x}{2|a|} \left[\coth(Pe_h) - \frac{1}{Pe_h} \right]$$

The term in brackets in the above definition of τ approaches 0 when Pe_h approaches 0 and approaches 1 when Pe_h approaches infinity. Thus, this allows us to transition from the diffusion formulation to the convection formulation depending on Pe_h.

Using the above definition of τ and the procedure used for the wave equation (Section 7.2), we obtain the restriction operator shown below.

Table 5
Results for the 1-D first order wave equation.

Implementation	Damping factor
SUPG restriction	0.3800
Standard restriction	0.9578
p-Multigrid, $p = 1$ to $p = 0$	0.3333

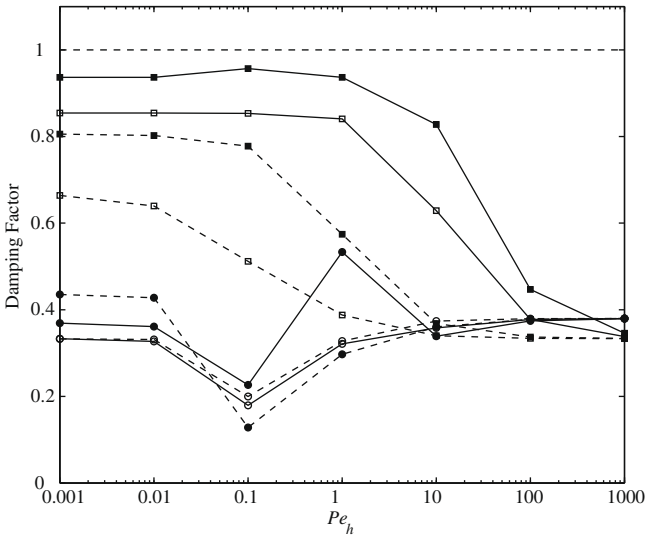

Fig. 3. Damping factors for the CD equation using a transition from $p = 1$ DG to $p = 1$ SUPG (circles) and DG $p = 1$ to 0 (squares). Open markers correspond to the Bassi et al. scheme and closed markers correspond to the LDG schemes. Dashed lines correspond to η/η_0 equal to one and solid lines to η/η_0 equal to four. $\omega = 2/3$ in every case.

$$I^T_{SUPG} = \begin{bmatrix} \cdots & 0 & [\cdots & \mathbf{V} & \cdots &] & 0 & \cdots & \\ & \cdots & 0 & [\cdots & \mathbf{V} & \cdots &] & 0 & \cdots \end{bmatrix}_{N\times 2N} \tag{22}$$

where $[\cdots \quad \mathbf{V} \quad \cdots] = [\tau \quad 1+\tau \quad 1-\tau \quad -\tau]$

As in Section 7.2, because the trial functions are constrained to be piecewise continuous, we again use the prolongation operator defined in Eq. (8).

7.5. DG to SUPG results for the convection–diffusion equation

Fig. 3 is a plot of the damping factors versus Pe_h for the Bassi et al. and LDG schemes using the DG to SUPG multigrid transition shown with the circle markers (○,●). For comparison, we also plot with square markers (□,■) the damping factors for the schemes using a DG $p = 1$ to 0 transition. The data with the open markers (○,□) and closed markers (●,■) correspond to the Bassi et al. scheme and the LDG schemes, respectively. All results are given for η/η_0 equal to one (dashed lines) and four

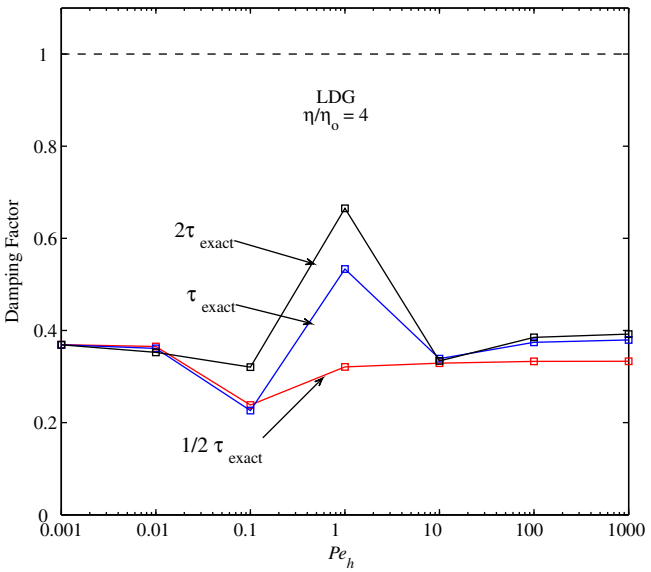

Fig. 4. Variation in damping factors for the LDG, $\beta = 0$ scheme with $\eta/\eta_o = 4$ and using inexact values of τ.

(solid lines). The broken horizontal line at $y = 1$ indicates graphically the level below which the damping factors must lie for a scheme to be stable. We see that with the DG to SUPG multigrid transition, all schemes converge rapidly over the entire range of Pe_h. Also, as Pe_h increases (more convective processes), the damping factors approach 0.3800; the damping factor for the case of pure convection (Table 5). Similarly, for smaller values of Pe_h (more diffusive processes), the damping factors approach that for the case of pure diffusion (Table 3). This implies that the new method of restriction is correctly transitioning from DG to continuous upwind discretization or standard Galerkin as warranted by the problem. The schemes with DG to SUPG multigrid transition show a significant improvement over those with DG $p = 1$ to 0 transition for $Pe_h \leqslant 10$. For $Pe_h \geqslant 10$, the DG to SUPG and DG $p = 1$ to 0 multigrid schemes perform comparably.

We also study the sensitivity of the DG to SUPG multigrid method to the upwind parameter τ. This is important because in multiple dimensions and on unstructured or stretched meshes, the fluid velocity and element length are not constant in different directions. Hence the exact value of τ may be difficult to define. Fig. 4 plots the damping factors versus Pe_h for the LDG, $\beta = 0$ scheme with $\eta/\eta_o = 4$. The three curves represent the damping factors for the scheme using upwind parameter τ_{exact}, $\frac{1}{2}\tau_{exact}$ and $2.0\tau_{exact}$, where $\tau_{exact} \equiv \tau$ as defined in Eq. (21). For $Pe_h \gg 1$ or $Pe_h \ll 1$, the results are fairly insensitive to the precise value of τ. For Pe_h of $O(1)$, there is a greater sensitivity to value of τ chosen. For the case with $\tau = \frac{1}{2}\tau_{exact}$, we actually see improved performance for most conditions. These characteristics are common to all schemes we have investigated.

8. Conclusions

We have shown that a p-multigrid algorithm that restricts to a $p = 1$ continuous space, although effective for DG discretizations of diffusive problems, fails when applied to the convection–diffusion equation. The reason for the failure is that for the wave equation, the transition to a first order continuous space results in central-difference equations in the coarser space. This difficulty cannot be eliminated by simply rediscretizing using an upwind operator in the coarse space; The damping factors obtained by using standard operators to restrict to the continuous space and then using an upwind discretization on the coarse space were poor.

The above difficulty has been resolved using ideas from the SUPG formulation [18] to modify the restriction operator. When the modified restriction operator is applied to the wave equation an upwind discretization is obtained on the continuous space. The modified method essentially uses an upwind weighted restriction operator, which to our knowledge, has never been applied before in a p-multigrid context. This new approach proved to be an effective p-multigrid strategy for the wave equation and was then generalized to the convection–diffusion equation using the SUPG upwind parameter, τ. The generalized approach was effective for all values of the grid Peclet number, Pe_h.

References

[1] E.M. Ronquist, A.T. Patera, Spectral element multigrid I: formulation and numerical results, SIAM Journal on Scientific Computing 2 (4) (1987) 389–406.
[2] K. Hillewaert, N. Chevaugeon, P. Geuzaine, J.-F. Remacle, Hierarchic multigrid iteration strategy for the discontinuous Galerkin solution of the steady Euler equations, International Journal for Numerical Methods in Fluids 51 (9–10) (2006) 1157–1176.
[3] K. Brix, M.C. Pinto, W. Dahmen, A Multilevel Preconditioner for the Interior Penalty Discontinuous Galerkin Method, Tech. Rep., Institut für Geometrie und Praktische Mathematik, RWTH Aachen, July 2007.
[4] B.T. Helenbrook, D. Mavriplis, H. Atkins, Analysis of p-Multigrid for continuous and discontinuous finite element discretizations, in: The 16th AIAA Computational Fluid Dynamics Conference, AIAA-2003-3989, Orlando, Florida, June 2003.
[5] B.T. Helenbrook, H. Atkins, Application of p-multigrid to discontinuous Galerkin formulations of the Poisson equation, AIAA Journal 44 (3) (2005) 566–575.
[6] B.T. Helenbrook, H.L. Atkins, Solving discontinuous Galerkin formulations of Poisson's equation using geometric and p-multigrid, AIAA Journal 46 (4) (2008) 894–902.
[7] K.J. Fidkowski, T.A. Oliver, J. Lu, D.L. Darmofal, p-Multigrid solution of high-order discontinuous Galerkin discretizations of the compressible Navier–Stokes equations, Journal of Computational Physics 207 (1) (2005) 92–113.
[8] T.A. Oliver, Multigrid Solution for High-Order Discontinuous Galerkin Discretizations of the Compressible Navier–Stokes Equations, Master's thesis, Massachusetts Institute of Technology, 2004.
[9] H. Luo, J.D. Baum, R. Lohner, A p-multigrid discontinuous Galerkin method for the euler equations on unstructured grids, Journal of Computational Physics 211 (2) (2006) 767–783.
[10] B.S. Mascarenhas, B.T. Helenbrook, H.L. Atkins, Application of p-multigrid to discontinuous Galerkin formulations of the Euler equation, AIAA Journal 47 (5) (2009).
[11] D.N. Arnold, F. Brezzi, B. Cockburn, L.D. Marini, Unified analysis of discontinuous Galerkin methods for elliptic problems, SIAM Journal on Numerical Analysis 39 (5) (2002) 1749–1779.
[12] B. Cockburn, C.-W. Shu, The local discontinuous Galerkin method for time-dependent convection–diffusion systems, SIAM Journal on Numerical Analysis 35 (6) (1998) 2440–2463.
[13] F. Bassi, S. Rebay, G. Mariotti, S. Pedinotti, M. Savini, A high-order accurate discontinuous finite element method for inviscid and viscous turbomachinery flows, in: R. Decuypere, G. Dibelius (Eds.), Proceedings of the Second European Conference on Turbomachinery, Fluid Dynamics, and Thermodynamics, Technologisch Instituut, Antwerpen, Belgium, 1997, pp. 99–108.
[14] C.R. Nastase, D.J. Mavriplis, High-order discontinuous Galerkin methods using a spectral multigrid approach, in: 43rd AIAA Aerospace Sciences Meeting and Exhibit – Meeting Papers, 2005, pp. 4885–4896.
[15] H. Luo, J.D. Baum, R. Lohner, A fast p-multigrid discontinuous Galerkin method for compressible flows at all speeds, AIAA Journal 46 (3) (2008) 635–652.
[16] K.V. Den Abeele, T. Broeckhoven, C. Lancor, Dissipation properties of the 1D spectral volume method and application to a p-multigrid algorithm, Journal of Computational Physics 224 (2) (2007) 616–636.
[17] Finite Element Methods for Convection Dominated Flows. American Society of Mechanical Engineers, Applied Mechanics Division, AMD, vol. 34, 1979.
[18] A. Brooks, T. Hughes, Streamline upwind/Petrov Galerkin formulations for convection dominated flows with particular emphasis on the incompressible Navier–Stokes equations, Computer Methods in Applied Mechanics and Engineering 32 (1982) 199–259.

[19] T.J.R. Hughes, M. Mallet, A new finite element formulation for computational fluid dynamics: III. The generalized streamline operator for multidimensional advective diffusive systems, Computer Methods in Applied Mechanics and Engineering 58 (1986) 305–328.
[20] M.P. Leclercq, B. Stoufflet, Characteristic multigrid method application to solve the Euler equations with unstructured and unnested grids, Journal of Computational Physics 104 (2) (1993) 329–346.
[21] B. Koren, P. Hemker, Damped, direction-dependent multigrid for hypersonic flow computations, Applied Numerical Mathematics 7 (4) (1991) 309–328.